



INSTITUTE FOR DEFENSE ANALYSES

**CLEARED**  
**For Open Publication**

Nov 27, 2023

Department of Defense  
OFFICE OF PREPUBLICATION AND SECURITY REVIEW

## **On the Risk of Kessler Syndrome: A Statistical Modeling Framework for Orbital Debris Growth**

Cameron J. Liang, Principal Author  
Paul E. Fanto  
Angelo J. Signoracci

October 2023  
IDA Report 3000897

**Approved for Public Release**

INSTITUTE FOR DEFENSE ANALYSES  
730 East Glebe Road  
Alexandria, Virginia 22305



The Institute for Defense Analyses is a nonprofit corporation that operates three Federally Funded Research and Development Centers. Its mission is to answer the most challenging U.S. security and science policy questions with objective analysis, leveraging extraordinary scientific, technical, and analytic expertise.

### **About This Publication**

This work was conducted by the IDA Systems and Analyses Center under contract HQ0034-19-D-0001, Project AX-1-3100, “Technical Analysis for the Director, Developmental Test, Evaluation, and Assessments,” for the Director, Developmental Test, Evaluation, and Assessments (D(DTE&A)). The views, opinions, and findings should not be construed as representing the official position of either the Department of Defense or the sponsoring organization.

Approved for Public Release.

### **Acknowledgments**

The authors would like to thank the IDA review committee, Dr. Stephen Ouellette (chair), Dr. Jennifer L. Bewley, Dr. Peter M. Mancini, Dr. Daniel L. Pechkis, and Dr. James D. Thorne, for providing technical review of this effort.

### **For More Information**

John S. Hong, Project Leader  
jhong@ida.org, (703) 845-2564

Stephen M. Ouellette Director, SED  
souellet@ida.org, (703) 845-2443

### **Copyright Notice**

© 2023 Institute for Defense Analyses  
730 East Glebe Road, Alexandria, Virginia 22305 • (703) 845-2000

This material may be reproduced by or for the U.S. Government pursuant to the copyright license under the clause at DFARS 252.227-7013 (Feb. 2014).

**CLEARED**  
**For Open Publication**

Nov 27, 2023

Department of Defense  
OFFICE OF PREPUBLICATION AND SECURITY REVIEW

# On the Risk of Kessler Syndrome: A Statistical Modeling Framework for Orbital Debris Growth

Cameron Liang<sup>†</sup>, Paul Fanto<sup>†</sup> and Angelo Signoracci<sup>†</sup>

System Evaluation Division, Institute for Defense Analyses, 730 E  
Glebe Rd, Alexandria, 22305, VA, USA.

Contributing authors: [cliang@ida.org](mailto:cliang@ida.org); [pfanto@ida.org](mailto:pfanto@ida.org);  
[assignora@ida.org](mailto:assignora@ida.org);

<sup>†</sup>These authors contributed equally to this work.

## Abstract

We present a statistical framework for modeling the evolution of orbital debris and the risk of the runaway debris growth, commonly known as the Kessler Syndrome. The framework builds upon traditional Particle in the Box (PIB) models with sources and sinks for the relevant orbital debris processes. In contrast to PIB models that typically provide a single trajectory for the evolution of the system, we stochastically sample a range of trajectories representing possible evolutionary paths, given the underlying source-sink rates. With this statistical framework, we provide a measure for risk of exponential runaway growth,  $\mathbf{P}_{\mathbf{Exp}}$ , defined as the fraction of trajectories that have produced runaway growth. We show that this parameter is sensitive to debris generation in collisions, satellite de-orbit rules and debris injection events (e.g., anti-satellite tests). For a certain set of parameters, we also show that there exists an unstable equilibrium absent in the traditional deterministic models.

**Keywords:** Kessler Syndrome, Orbital Debris

# 1 Introduction

The space environment is changing rapidly as governments and commercial entities launch increasing numbers of payloads into Earth orbit, primarily low Earth orbit (LEO). Data from [space-track.org](https://space-track.org) [1], the data sharing website of the 18th Space Defense Squadron (18th SDS), shows that the rate of payloads launched into orbit has risen from roughly 300 per year in 2018 to roughly 1500 per year currently. Commercial mega-constellations, such as Space-X's Starlink, already have thousands of satellites in orbit and, according to current plans, will ultimately consist of many more. It is important to understand the operational risks to spacecrafts, and how they can coexist as the space environment gets increasingly more crowded.

In particular, as the number of payloads in orbit increases, risk of producing orbital debris through explosions or collisions increases. In 1978, Kessler and Cour-Palais identified the risk of a self-sustaining process of collisions fed by increasing satellite launches, commonly referred to as the “Kessler syndrome” [2]. If such a process grows out of control, it could render parts of the Earth orbital environment inoperable. Consequently, predictive modeling of the orbital environment is useful to guide policy and practical decision making in the near future.

There are two primary classes of models that address long-term orbital debris evolution. One class updates the positions of all current objects dynamically with high fidelity propagators and randomly samples collisions among objects that come into close conjunction. Examples of such models are NASA's LEGEND model [3] and the DAMAGE model [4]. Monte Carlo runs from these models are used to capture the statistical variation in the collisions and are particularly useful for the assessment of near-term collision risk. However, these models have tended to underpredict debris evolution, mainly because they do not account for rare events that produce large numbers of debris. Furthermore, the models are computationally intensive, making it challenging to use them for parameter sensitivity studies.

The other class of models are source-sink evolutionary models, sometimes called particle-in-the-box (PIB) models. These models consist of a set of species (e.g., satellites, debris) that interact via a set of processes (e.g., launch, decay, collisions) that operate at various average rates. The model then updates the species population via a set of coupled ordinary differential equations (ODEs). Examples of these sorts of models are Lotka-Volterra models of predator-prey systems and SIR<sup>1</sup> models of disease spread. Example evolutionary models for orbital debris are the MOCAT family of models [5–8], the model of Somma [9], the FADE model [10], and the model of Talent [11]. These fast-running models can provide insight on the effects of various parameters on the orbital environment, but they lack the detailed physics included in the high-fidelity propagation models like LEGEND.

---

<sup>1</sup>SIR stands for Susceptible, Infected, and Recovered

However, the evolutionary models as currently applied do not provide insight into the full range of possible outcomes that could be generated by the model processes because they generally do not account for the randomness of collisions. To understand this range, one can use stochastic source-sink evolutionary models. Stochastic models beyond mean-field theory are widely applied in physics [12], cell biology [13–15], epidemiology [16–18], evolutionary biology and ecology [19, 20], and chemistry [21–24]. Instead of solving for a single trajectory (i.e., time evolution of the quantity of interests) for the system, these models solve for a time-dependent probability distribution governing all possible states of the system. The equation that determines this probability distribution is known as the Master Equation [25] and is typically unfeasible to solve exactly. Practical models using the Master Equation formalism generate a large set of trajectories and extract statistical information from these samples. For example, stochastic models can quantify the chance of the system evolving to a certain state, given a set of control parameters. These models can therefore be useful for understanding the risk of encountering runaway debris growth under certain environmental conditions.

Here, we develop a simple stochastic evolutionary model for the orbital environment. This model mainly demonstrates how stochastic evolutionary models can apply to the study of orbital debris production. Similar to many evolutionary models in literature, it consists of satellite and debris populations evolving under launch, decay, explosion, and collision processes. We implement stochastic sampling methods to generate system trajectories given underlying rates for these processes. We then show how the trajectory distribution changes for various sets of model parameters. Furthermore, one can define conditions indicating when a trajectory has reached runaway growth and quantify the risk of runaway growth in each simulation. We show how this runaway growth risk changes with launch rate, decay rate, and the number of debris produced per collision. We also investigate the sensitivity of the system to an injection of orbital debris at a certain time, representing, e.g., the effect of an anti-satellite (ASAT) test. Finally, we outline future directions for improving our model.

This paper is organized as follows. In Sec. 2, we describe our stochastic sampling model of the orbital debris environment. In Sec. 3, we show how the range of environmental outcomes in our model changes as a function of various model parameters. Finally, in Sec. 4, we summarize our results and discuss directions for future study.

## 2 Methodology

### 2.1 Statistical Framework

The central object in an evolutionary source-sink model is the population vector  $\mathbf{N}(t)$  representing the numbers of objects of various species at a given time  $t$ . In an orbital evolutionary model, species can be indexed by object type (satellite and debris), length scale, altitude, and other parameters. The model

also consists of a rate matrix  $\mathbf{\Omega}$  that governs how the state changes with time. These rates can be state- and time-dependent.

Typical evolutionary models propagate the population vector  $\mathbf{N}$  over a series of time steps, producing a single trajectory for each species. However, given the underlying rates, several different system trajectories are possible. The time-dependent probability distribution  $\mathbf{P}_{\mathbf{N}}(t)$  encapsulates the range of possible population values at time  $t$ . This probability distribution's evolution follows the Master Equation [25]

$$\frac{d\mathbf{P}_{\mathbf{N}}}{dt} = \mathbf{\Omega}\mathbf{P}_{\mathbf{N}}(t) \quad (1)$$

Propagating this equation provides information on the full range of system states with time. In practice, the number of possible system states is so large that solving Eq. (1) exactly becomes unfeasible. Instead, we approximate  $\mathbf{P}_{\mathbf{N}}$  by stochastically sampling system trajectories, as described in more detail in Sec. 2.3.

## 2.2 Orbital Environment Model

In this paper, we implement a simple stochastic model of the orbital environment similar to other models in the literature [5–11]. Our main goal is to use a simple model to illustrate the advantages of the stochastic source-sink method. Further development of the model (e.g., including altitude-dependent rates) will be the subject of future work.

Our toy model consists of two species of objects: active satellites and debris.<sup>2</sup> The model also assigns a set of length scales to each object species. Thus, the population vector elements can be written as  $N_{\alpha, \ell_i^\alpha}$ , where  $\alpha = (\text{sat}, \text{deb})$  labels the object species and  $\ell_i^\alpha$  ( $i = 1, \dots, n_\ell^\alpha$ ) is the length scales. The total dimension of the population vector is therefore  $n_\ell^{\text{sat}} + n_\ell^{\text{deb}}$ .

The model includes four processes that change the state of the system: launch, decay, collisions, and explosions. We describe the rates and changes to the population vector for each process in the following sections.

### 2.2.1 Launch

The number of launch events per unit time is generally referred to as the launch rate. However, the number of payloads can vary significantly across global launch sites. For our model, the number of satellites launched per year is the relevant source term for debris production. They can be a source of debris upon collisions or explosions as described in latter subsections. At the moment, we do not model derelict satellites and they do not contribute to the population. Therefore, we have chosen not to model the launch events per unit time and number of payloads per launch event separately. Instead, for simplicity, we define “launch rate” as the number of satellites added to space due to launches. We designate the total launch rate by  $\Omega_L$ .

---

<sup>2</sup>We do not explicitly include derelict satellites, as is done in, e.g., [5–7].

Another relevant factor is the initial mass or size of the satellites. The satellite size determines the number of debris pieces produced by a satellite breakup via an explosion or collision. As done in other models [3, 5–7, 9], we assume a one-to-one conversion between the mass and length scale. With this assumption, we can describe the resulting debris distribution from satellite breakup as a function of debris length scale (e.g., by using NASA Standard Breakup Model [26]). We therefore assign a length scale  $\ell_i^{\text{sat}}$  to each satellite launched into the space environment.<sup>3</sup>

### 2.2.2 Decay

We model decay rates of satellites and debris as they are removed from the system. The details of removal mechanisms are not modeled (e.g., atmospheric density and its drag forces). At this stage, we use free parameters to control the decay rates to generically incorporate mechanisms such as Post Mission Disposals (PMD) of satellites or Active Debris Removal (ADR). If all satellites behave the same rate (similarly for debris), the decay rate for a species varies linearly with the number of objects in the system:

$$\omega_{D,\alpha,\ell_i^\alpha}(t) = r_{D,\alpha} N_{\alpha,\ell_i^\alpha}(t) \quad (2)$$

where  $\alpha$  indicates the object type (satellite or debris) and  $\ell_i^\alpha$  is the length scale, with  $i$  indexing the possible choices. In our current model, we may choose different decay rate factors  $r_{D,\text{sat}}, r_{D,\text{deb}}$  for satellites and debris, respectively. The former can be interpreted as planned de-orbiting rate (i.e., PMD) and the latter represents a timescale that one can choose to remove debris in addition to natural decay (i.e., ADR). However, we note that our current model does not reflect the variation in decay rates due to different area-to-mass ratios of objects and their orbital altitudes.

### 2.2.3 Explosions

Payload explosions can add debris to the environment. We assume that each satellite has a fixed probability of exploding in each time interval. Consequently, the rate of explosions varies linearly with the number of satellites:

$$\omega_{E,\text{sat},\ell_i^{\text{sat}}}(t) = r_E N_{\text{sat},\ell_i^{\text{sat}}}(t) \quad (3)$$

Our model uses the NASA Standard Breakup Model (SBM) [26] to determine debris production from explosions. Specifically, the number of debris produced with length scales at or greater than a specific length  $\ell$  (in unit of m) is:

$$n_{\text{deb}}(\ell' > \ell) = 6s\ell^{-1.6} \quad (4)$$

where  $s$  is a scale factor and typically set to one. The likelihood of explosions are slowly decreasing in recent years. While we include the descriptions for

---

<sup>3</sup> $i = 1, \dots, n_\ell^{\text{sat}}$  indexes the possible choices for satellite length scale; see the introduction to Sec. 2.1.

how explosion of satellites are generating debris, we have set the explosion rate to zero to focus the study on other parameters (Sec. 3).

### 2.2.4 Collisions

Collisions are the most significant potential source of debris. Our model includes all possible collisions: satellite-satellite, satellite-debris, and debris-debris. As with any two-body interaction, the total rate of collisions can be expressed as a quadratic function of the total number of objects on orbit:

$$\Omega_C(t) = r_C N_{\text{tot}}^2(t) \quad (5)$$

where  $N_{\text{tot}}$  is the total number of all satellites and debris for all length scales. The coefficient  $r_C$  is typically computed assuming the kinetic theory of gas [11, 27],

$$r_C = \frac{\pi v_r}{2 V} A_{\text{cross}} = p A_{\text{cross}} \quad (6)$$

where  $p = \frac{\pi v_r}{2 V}$  is often described as the intrinsic collision probability,  $v_r$  is the averaged collision velocities (in the order of 10 km/s),  $V$  is the volume of interest (e.g.,  $\sim 12$  cubic km for LEO), and  $A_{\text{cross}}$  is the averaged collisional cross section [9]. Given a collisional cross section of  $1 \text{ m}^2$ , an order of magnitude estimate for  $r_C$  is  $10^{-10} \text{ yr}^{-1}$  in the volume of LEO. Given satellites are not in random motion, the kinetic theory of gas assumption is not entirely correct. Some authors have introduced a multiplicative factor to correct for this approximation [11]. With  $r_C$  and  $N_{\text{tot}}$ , one can calculate an average rate of collisions among all objects.

Once the total collision rate at a given time step is given, one has to determine the relative rates for the various collision types (e.g., satellite-satellite, satellite-debris, debris-debris). These relative collision rates will ultimately determine the numbers and sizes of debris produced. The relative collision rate between objects of type  $\alpha$  and length scale  $\ell_i^\alpha$  and objects of type  $\beta$  and length scale  $\ell_j^\beta$  is proportional to the product of the collisional cross-section of the objects and their population. Specifically, this relative collision rate  $\omega_{\alpha\ell_i^\alpha, \beta\ell_j^\beta}^C$  is given by:

$$\omega_{\alpha\ell_i^\alpha, \beta\ell_j^\beta}^C \propto (\ell_i^\alpha + \ell_j^\beta)^2 N_{\alpha\ell_i^\alpha} (N_{\beta\ell_j^\beta} - \delta_{\alpha,\beta} \delta_{i,j}) \quad (7)$$

where the delta function covers the case of two objects of the same species colliding. We normalize the relative rates so that their sum equals the total rate in Eq. (5).

Our model includes a lethal debris length scale,  $\ell_{\text{lethal}}$ . This is used as a proxy for the mass and kinetic energy threshold for the lethality of objects [26]. Debris objects with lengths below the lethal length scale cannot cause catastrophic collisions, which we define as events that generate debris. For the current study, this is a free parameter and is chosen to be 5 cm to reflect the typical lower limit of the observable size of objects in LEO. However, the actual lethal length scale is believed to be smaller. Scaling this parameter will change

the number of lethal debris produced per collisions according to a breakup model (e.g., the NASA breakup model). While constraining the value of  $\ell_{\text{lethal}}$  is outside the scope of our current study, observations that measure  $\ell_{\text{lethal}}$  can provide a key ingredient for the long-term debris evolutionary growth modeling.

As with explosions, the model uses the NASA SBM to model debris production from collisions. The SBM model for the number of debris above a given length scale  $\ell$  (in units of m) generated by a catastrophic collision is:

$$n_{\text{deb}}(\ell' > \ell) = 0.1(M_1 + M_2)^{0.75} \ell^{-1.71} \quad (8)$$

where  $M_{1,2}$  are the masses (in units of kg) of the two objects involved in the collision. We calculate the mass for each object as the area divided by the area-to-mass ratio (AMR). The SBM relates the area to a length scale and provides a distribution of the AMR [26]. Thus, drawing the masses of the objects adds another form of stochasticity to our model.

## 2.3 Stochastic Sampling

The Master Equation (1) is a vector equation where the length of the vector equals the number of possible states of the system. This number of different populations is astronomically large. Therefore, it is unfeasible to solve Eq. (1) directly for all but the simplest models. However, it is possible to approximate the time-dependent probability distribution  $\mathbf{P}_{\mathbf{N}}$  by Monte Carlo sampling a large number of system trajectories. The Gillespie algorithm [21], originally developed to model chemical reactions, provides a method for this Monte Carlo sampling. Using the process rates, this algorithm randomly generates time steps to events (i.e., launch, decay, collision, explosion) and which event occurs at each time.

For the Gillespie algorithm, the sampling time step varies and is inversely proportional to the total rate for all processes. In the present problem in exploring the Kessler Syndrome where collision rates can grow unbounded, even such a sampling algorithm would slow down the Monte Carlo simulation dramatically as increasing process rates cause diminishing time steps. In the calculations presented below, we implement an approximate form of the Gillespie algorithm: the tau-leaping method [22, 23]. In this approach, one can select a constant time step  $\tau$ , and generate the events in the time interval  $(t, t + \tau)$  from Poisson distributions. This approximation assumes that the process rates do not change much in the time interval  $\tau$ . The mean number of events in the time interval is given by  $\Omega\tau$ , where  $\Omega$  is given by the process rates described in the previous section.

## 2.4 Risk of Exponential Growth

Given a set of fixed model parameters, the trajectories obtained by the stochastic sampling method enable us to understand the likelihood of various system

outcomes. The probability or risk of an outcome by a certain time is given by the fraction of trajectories in which this outcome has occurred by this time. In studying the Earth orbital environment, we are particularly interested in the risk of runaway debris growth rendering the environment inoperable. A trajectory is of concern when the number of debris exceeds a high threshold<sup>4</sup> and is increasing quickly. For these trajectories, we define the time of exponential growth onset ( $t_{\text{Exp}}$ ) when the logarithmic growth of debris experiences the steepest increase as the natural characteristic timescale,

$$t_{\text{Exp}} = \text{argmax} \left( \frac{d \ln N_{\text{deb}}}{dt} \right) \quad (9)$$

For example, Figure 1 shows the growth of debris in one simulated trajectory and the corresponding logarithmic gradient, where  $t_{\text{Exp}}$  is defined according to our definition.

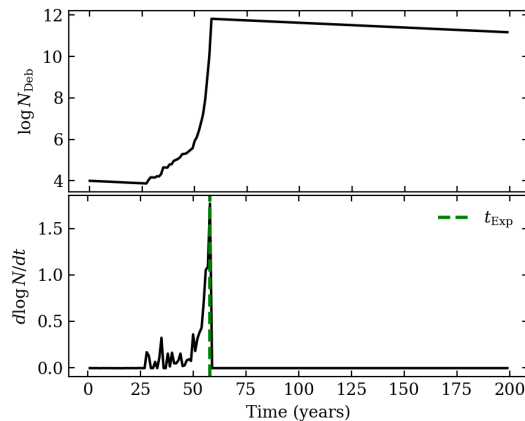


**Fig. 1** Example of a debris growth with launch at 1500 payloads per year, satellite decay and debris decay rate 1/25 and 1/95 per year. Collision coefficient  $r_C = 1.77 \times 10^{-10} \text{ yr}^{-1}$

Over an ensemble of simulated trajectories, we define the risk of exponential debris growth by time  $t$  as the fraction of simulated trajectories that have undergone exponential growth,  $P_{\text{Exp}}(t) \equiv n_{\text{Exp}}(t)/n_{\text{total}}$ . This can be computed simply by counting the number of trajectories that have undergone exponential growth before time  $t$ :

$$P_{\text{Exp}}(t_{\text{Exp}} \leq t) = \frac{1}{n_{\text{total}}} \sum_{i=1}^{n_{\text{total}}} \Theta(t - t_{\text{Exp}}) \Theta(n_{\text{deb}} - n_{\text{deb}}^{\text{thresh}}), \quad (10)$$

<sup>4</sup>In practice, a threshold is chosen to select trajectories that have undergone exponential growth. The outcome is not sensitive to the choice of this threshold.

where  $n_{\text{total}}$  is the total number of simulated trajectories,  $n_{\text{deb}}^{\text{thresh}}$  is the threshold value used to filter out trajectories in which runaway debris growth has not occurred, and  $\Theta(x)$  is the Heaviside step function

$$\Theta(x) = \begin{cases} 1 & x \geq 0 \\ 0 & x < 0 \end{cases} \quad (11)$$

In other words, the summation simply counts the number of trajectories which has debris greater than a threshold and is experiencing dramatic growth. The risk metric  $P_{\text{Exp}}$  in Eq. (10) approximates the probability of runaway growth, which we sometimes call the risk of Kessler Syndrome. This risk would be given exactly by the integral over the Master-Equation probability distribution  $\mathbf{P}_{\mathbf{N}}$ . The accuracy of this approximation increases with the number of sampled trajectories.

### 3 Results

In this section, we apply our model to illustrate how various model parameters change the risk of runaway debris growth  $P_{\text{Exp}}$ . In particular, we examine the effect of different numbers of debris produced per collision, launch rate, satellite de-orbit rate, and debris decay rate. Finally, we examine the effect of an injection of debris pieces at a certain time, representing, e.g., an ASAT test.

Although we included explosion rates in our model for completeness, we set the explosion rate to zero in all the examples below.

#### 3.1 Effects of Fragmentation Amplitude

Reducing the amount of lethal debris that a satellite produces upon breakup would mitigate debris growth. In particular, designing spacecrafts with limited lethal debris produced and validating these designs in developmental and operational testing [28] could improve the long-term sustainability of space. In this section, we apply our model to describe the effects of differences in spacecraft design and breakup properties on the orbital environment.

Most debris growth models use the NASA SBM [26] to describe the debris distribution produced by collisions. To allow for the production of varying numbers of debris, we treat the total number of debris ( $\Delta N_{\text{deb}}$ ) as a free parameter while preserving the shape of the SBM debris size distribution. Specifically, we apply a rescaling<sup>5</sup>

$$n_{\text{deb}}(\ell) = \frac{\Delta N_{\text{deb}}}{\sum_{\ell_{\min}}^{\ell_{\max}} n_{\text{SBM}}(\ell)} n_{\text{SBM}}(\ell) \quad (12)$$

where  $n_{\text{SBM}}(\ell)$  is the size distribution of debris, derived from the cumulative size distribution in Eq. (8). The minimum debris size in the simulation

---

<sup>5</sup>We note that the NASA SBM distribution does not enforce conservation of mass. Therefore, applying a re-scaling does not violate any standard assumptions in our model.

$\ell_{\min}$  can be set to be equal to or below the lethal debris length  $\ell_{\text{lethal}}$ <sup>6</sup>. If  $\ell_{\min} < \ell_{\text{lethal}}$ , the number of lethal debris will eventually cascade down to the length scale smaller than  $\ell_{\text{lethal}}$  via collisional breakup. These “non-lethal” objects are tracked in our simulations but do not cause catastrophic collisions. Although they do not cause additional breakup, they might turn active satellite to derelict satellites. However, this effect is not included in the current study. The maximum size of the objects in our simulations is the size of the satellites.<sup>7</sup>

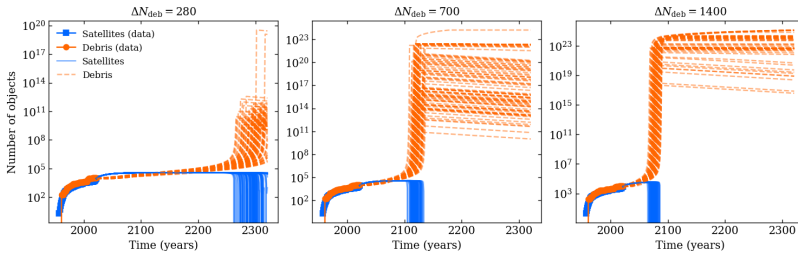


**Fig. 2** Satellites (blue lines) and debris (orange lines) numbers for various total numbers of debris produced per collision  $\Delta N_{\text{deb}}$ . The blue and orange points are historical data and serve as initial conditions for the simulations. The total collision rate parameter is  $r_C = 5.31 \times 10^{-10} \text{ yr}^{-1}$  in each case. The downturn of the blue line indicates nearly all satellites are destroyed corresponding the cascade of collisions that introduces the exponential growth of debris in the orange lines. After this happens, we turn off the launch of satellites, the debris decays according to the rate  $r_D$ .

Figure 2 shows the model results for three choices of the debris production amplitude  $\Delta N_{\text{deb}}$ . The launch rate is 1500 satellites per year in each case, which is roughly equal to the launch rate in recent years. We set the decay rate to be  $r_D = 1/95 \text{ yr}^{-1}$ , which is representative of the timescale for objects to decay from LEO (800-1000 km altitude). The blue and orange points in Figure 2 are the historical values for the number of cataloged satellites and debris taken from the public database by `space-track.org` [1]. These data points provide initial conditions for the simulations and are shown in all similar figures throughout this paper.

As shown in Figure 2, for each debris production amplitude, most simulations result in exponential debris growth given the aggressive launch rates and nominal decay rates. In these simulations, we turn off launch when exponential debris growth occurs (blue lines going to zero in the figures) as all satellites launched after this point would be immediately destroyed by debris. At this point, the debris numbers start to decay. Furthermore, collisions between debris populate the smaller size bins, eventually reaching the sizes below  $\ell_{\text{lethal}}$  that do not cause catastrophic collisions.

<sup>6</sup>Our goal is to explore the effects of  $\Delta N_{\text{deb}}$ , so we set  $\ell_{\text{lethal}} = 5 \text{ cm}$  for simplicity. We note that trackable debris are in the range of 5-10 cm in LEO. Variations in  $\ell_{\text{lethal}}$  do not change the qualitative results of the simulations.

<sup>7</sup>We have set this scale to a few meters. Note that increasing this length scale implies more massive satellite and would introduce additional debris.

Comparing the three scenarios, we note that a smaller debris production amplitude pushes the onset of exponential growth further into the future. Producing less debris per collision slows the rate at which the collisions can increase the numbers of debris, as expected. Figure 3 shows the risk parameter  $P_{\text{Exp}}$  as a function of time for the various total numbers of debris produced. The median of  $P_{\text{Exp}}$  moves from  $\sim 2300$  for  $\Delta N_{\text{deb}} = 280$  to  $\sim 2070$  for  $\Delta N_{\text{deb}} = 1400$ .

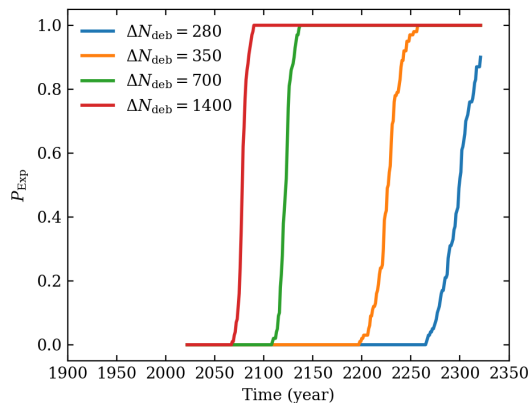


**Fig. 3** The probability of exponential debris growth  $P_{\text{Exp}}$  vs time for various debris production amplitudes. The simulation parameters are the same as in Figure 2.

### 3.2 Deorbit Rules and Unstable Equilibrium

The recent increase of launch rates, driven mainly by commercial entities (e.g., Space-X Starlink and OneWeb), has spurred a re-evaluation of the sustainability of space. In particular, the Federal Communications Commission (FCC) is re-evaluating the approval of thousands of launches by these commercial entities. Furthermore, the FCC has approved a change of the decades-old 25-year deadline for satellites to de-orbit to a 5-year rule recently [29]. Consequently, it is useful to quantify the impact of increased launch rates and new de-orbit rules on the risk of runaway debris growth.

In this section, we use our simple stochastic model to explore the effects on  $P_{\text{Exp}}$  of varying launch rates and satellite de-orbit rules, while keeping other parameters constant. Unlike in the simulations described in a previous section, we use here the NASA SBM without specifying the total number of debris produced. We again set the explosion rate to zero. In addition, we set the collision rate parameter to  $r_C = 1.77 \times 10^{-10} \text{ yr}^{-1}$ , which is consistent with the historical value<sup>8</sup> and the theoretical expectation in Eq (6) as described

<sup>8</sup>We estimate the average collision rate  $r_C = \langle N_{\text{coll}} \rangle / \langle N_{\text{tot}} \rangle^2$ , where  $\langle N_{\text{coll}} \rangle$  is the average number of collisions in the past 20 years, and  $\langle N_{\text{tot}} \rangle$  is the average number of objects in the same timeframe.

in Section 2. For de-orbiting satellites, the 25-year rule and the 5-year rule correspond to an average satellite de-orbit rate of  $1/25$  and  $1/5$  satellites per year, respectively<sup>9</sup>. For debris decay, since we model LEO as a single volume, we use an order-of-magnitude estimate  $r_{D,\text{deb}} = 1/95 \text{ yr}^{-1}$ . If a simulated trajectory of the debris experiences exponential growth, we shut off the satellite launches, which leads to an eventual decline of debris with the rate set by the debris decay rate.

Figures (4-6) show results from simulations with different satellite de-orbit rates. In particular, Figure (4) shows that, for an aggressive launch rate of 1500 per year and long de-orbit rule with a timescale of one hundred years, the model shows that runaway growth would likely occur in the 2050s.<sup>10</sup> But as the de-orbit timescale decreases, the onset time of runaway growth moves farther into the future, as shown in Figures (5) and (6). Given the stochasticity of the model, some simulated trajectories experience runaway growth as early as the 2050s, while others experience this growth much later, in the 2200s. Overall, reducing the allowed satellite lifetime before de-orbit pushes the distribution of exponential timescales farther out in time.

Interestingly, in Figure (6), majorities of the simulated trajectories remain stable even at late times. In this case, the de-orbit timescale is sufficiently short that collisions cannot effectively generate runaway growth. However, Figure (6) also shows that a small number of consecutive collisions can still kickstart the runaway growth<sup>11</sup>. This result acts like an unstable equilibrium solution; qualitatively similar to modeling in other fields [30], where background noise or parameter uncertainties can drive significantly different outcomes. Therefore, the uncertainty of model parameters, such as the collision rate parameters, should be observationally and/or theoretically constrained (see discussion section on the effects of collision rate). Nevertheless, this set of simulations shows that one can effectively reduce the risk of runaway debris growth dramatically by imposing a sufficiently short de-orbit timescale.

Figure (7) shows the change of  $P_{\text{Exp}}$  for the various satellite de-orbit rates investigated in the simulations described above. The 5-year rule is the only de-orbit rate that delays exponential growth far into the future. Nevertheless, one would like to drive  $P_{\text{Exp}}$  as close to zero as possible. Thus, in our current model, it seems that a launch rate of 1500 satellites per year is simply too high for space to be sustainable long-term, even with the 5-year rule in place.

However, we have assumed thus far that we have no control over the decay rate of debris. Active Debris Removal (ADR) techniques are currently being developed and could potentially reduce debris lifetimes, thereby reducing the risk of potential collisions [9]. To incorporate the effect of ADR in our model, we simply change the decay parameter  $r_{D,\text{deb}}$ . Figure (8) shows color maps of the risk parameter  $P_{\text{Exp}}$  at various times for a range of debris decay rates and satellite de-orbit rules. In Figure (8),  $P_{\text{Exp}}$  increases quickly with time in

---

<sup>9</sup>We assume that all satellites would comply with such rules.

<sup>10</sup>We do not consider results of our current model predictive yet, as the model is simple and has not been validated.

<sup>11</sup>Of course, this depends on the coupling of objects in space via the collision rate model.

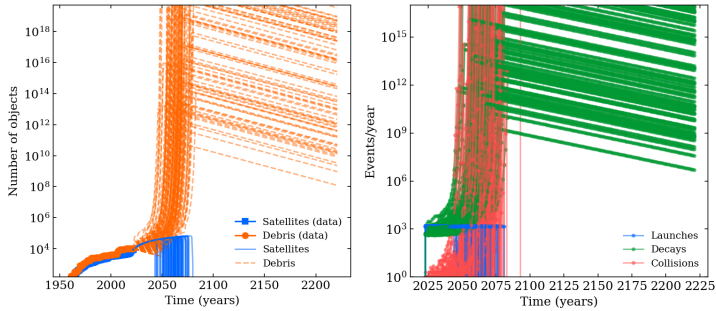


**Fig. 4** Satellite and debris numbers (left-hand figure) and numbers of events (right-hand panel) with a satellite launch rate of  $1500 \text{ yr}^{-1}$ , satellite de-orbit rate of  $r_D = 0.01 \text{ yr}^{-1}$ , the latter corresponds to a 100-year de-orbit rule on average.

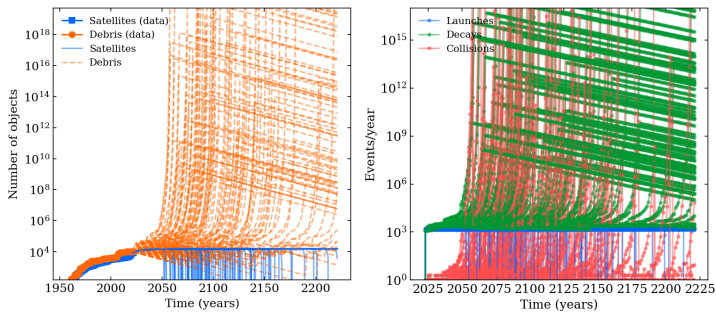


**Fig. 5** Same as Figure (4) with the same launch rate but with a satellite de-orbit rate of  $r_D = 0.04 \text{ yr}^{-1}$ , corresponding to a 25-year rule on average.

almost all cases. The 5-year rule is the only de-orbit rule that maintains low probability of runaway growth as late as 2082. However, even for the 5-year rule, the risk of runaway growth will continue to increase, as shown in Figure (7) above. However, if we reduce the launch rate to 300 satellites per year, which is in line with the historical launch rate before the recent increase, our model shows that the risk of runaway growth will remain low for a wide range of satellite and debris decay rates as far out as 2082, as shown in Figure 9. Figure (10) shows that, although the risk of exponential growth continues to grow for this lower launch rate, it never reaches 100%, and remains below 50% for the 5-year rule.

### 3.3 Effects of A Single Debris Injection Event

Sending weapons to destroy satellites is a growing concern for the growth of debris and sustainability of space. In particular, anti-satellite (ASAT) tests have been major contributors to recent orbital debris growth. Most recently, the 2007 Chinese ASAT test and 2021 Russian ASAT test have produced on the order of 1500-3000 trackable debris pieces [31]. Although a significant contribution to the debris population, it remains unclear quantitatively how

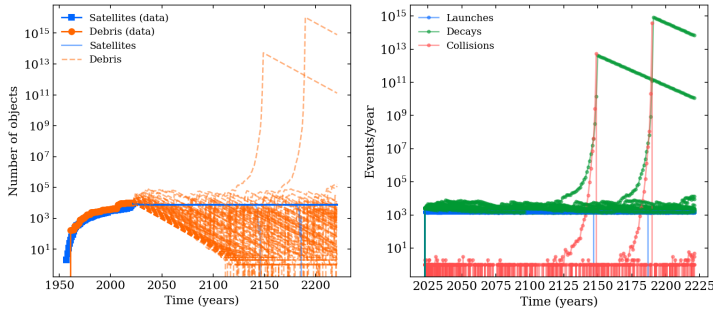


**Fig. 6** Same as Figure (4) with the same launch rate but with a satellite de-orbit rate of  $r_D = 0.2 \text{ yr}^{-1}$ , corresponding to a 5-year rule on average. There is low but non-zero risk of exponential growth given the decay rates are large enough. However, the simulation shows that a series of unfortunate, but possible, consecutive collisions can kick start the run-away growth as shown.

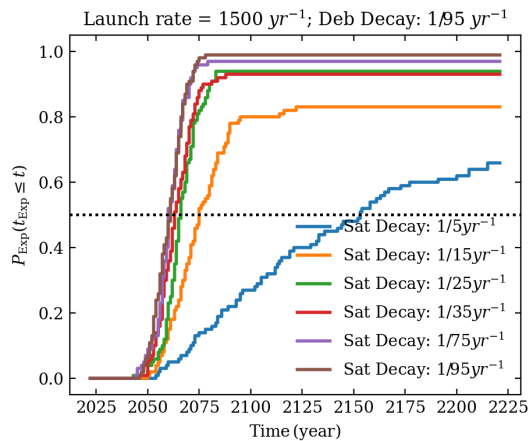


**Fig. 7**  $P_{\text{Exp}}$  vs time for various satellite de-orbit rules. The collision coefficient is set to  $r_C = 1.77 \times 10^{-10} \text{ yr}^{-1}$  and the launch rate is 1500 satellites per year.

these tests will change the risk of runaway debris growth over time. We can quantify the added risk of such debris injection events using our statistical framework. Specifically, we are interested in how an injection of debris will impact the probability of runaway growth  $P_{\text{Exp}}$ .

Injections of debris increase the collision probability by increasing the overall orbital population. Therefore, an injection of debris will impact the environment differently for different launch and decay rates. Figure (11) shows  $P_{\text{Exp}}$  results from three simulations for an injection of 1500 pieces of debris near the start of the simulation time and with varying debris decay rates. The launch rate was 1500 satellites per year in these simulations, consistent with launch behavior in recent years, and the collision rate factor was  $r_C = 1.77 \times 10^{-10} \text{ yr}^{-1}$ . Overall, we find that the injection increases  $P_{\text{Exp}}$

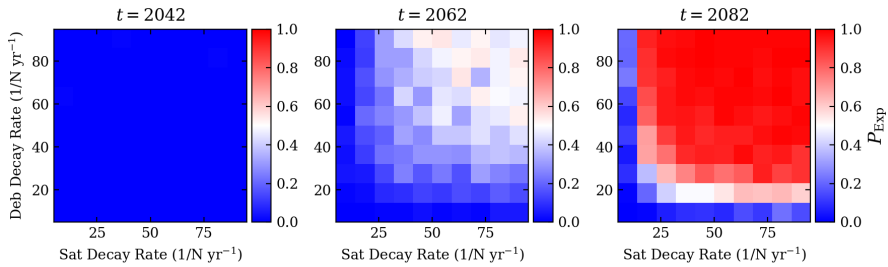


**Fig. 8** Modeling results for  $P_{\text{Exp}}$  at three time points with a launch rate of 1500 per year. We perform a parameter sweep for satellite and debris decay rates. The collision coefficient is  $r_C = 1.77 \times 10^{-10} \text{ yr}^{-1}$

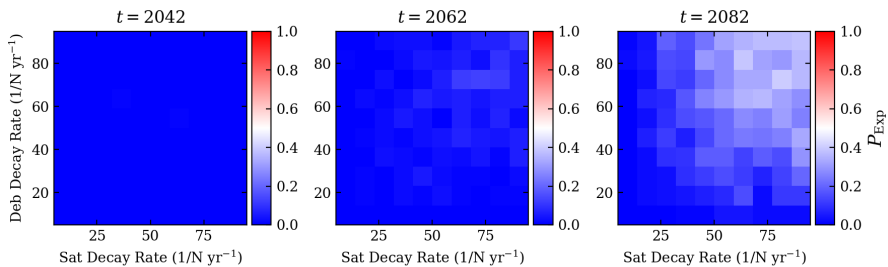


**Fig. 9** Modeling results with a launch rate of 300 satellites per year, with a collision coefficient  $r_C = 1.77 \times 10^{-10} \text{ yr}^{-1}$ . As one can see, the risk is greatly reduced as expected.

moderately after a few decades. For example, at the nominal debris decay rate  $r_D = 1/95 \text{ yr}^{-1}$ , the injection increases probability of runaway growth by roughly 10% at a given time compared with the control simulation without the injection. Equivalently, the injection of debris causes a given  $P_{\text{Exp}}$  to occur at an earlier time, compared with the simulation without the injection. For example, for the simulation with satellite de-orbit rate of  $1/25$  per year, the simulation without the injection reaches  $P_{\text{Exp}} \approx 20\%$  around 2150, while the simulation with injection reaches this risk value near the beginning of 2100. We also note that the effects of the injection will vary depending on the time of the injection and the state of the system (i.e., number of satellites and debris already in space).

These results support the U.S. commitment announced in April 2022 by Vice President Harris not to conduct destructive, direct-ascent anti-satellite missile testing and the subsequent push to establish that approach as a norm for responsible behavior in space, to maintain space sustainability [32]. The United Nations subsequently approved a draft resolution calling on all states not to conduct such tests [33, 34]. Additional simulations can assess the impact of debris-generating events, whether from destructive, direct-ascent anti-satellite missile testing or from other sources, and emphasize to what

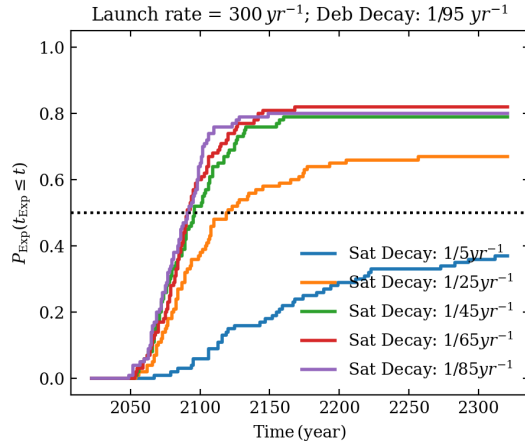


**Fig. 10**  $P_{\text{Exp}}$  vs time for various satellite de-orbit rules. The collision coefficient is set to  $r_C = 1.77 \times 10^{-10}$  and the launch rate is 300 satellites per year. Notice that  $P_{\text{Exp}}$  never reaches 1 on the timescales considered.

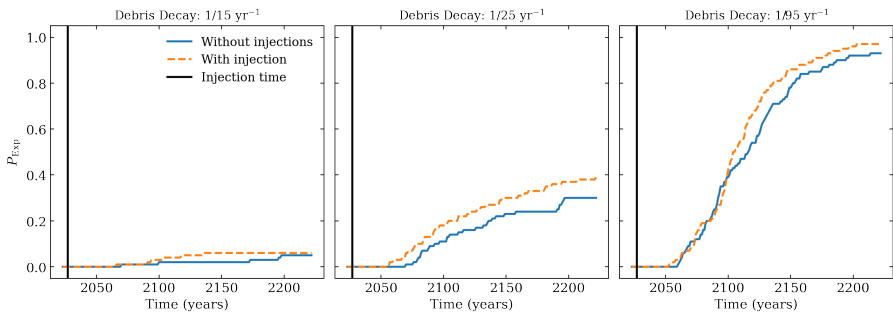


**Fig. 11** Comparison of  $P_{\text{Exp}}$  at three timesteps for simulations with and without a debris injection. The black vertical line indicate the year (2027) the debris is injected into the environment. The launch rate in these simulations is 1500 satellites per year. The collision coefficient is  $r_C = 1.77 \times 10^{-10} \text{ yr}^{-1}$ . The satellite decay rate is set to  $r_{D,\text{sat}} = 1/25 \text{ yr}^{-1}$ .

extent the norms for responsible behavior have to be extended to more comprehensive bans, such as eliminating all intentional kinetic effects against resident space objects.

## 4 Discussion and Conclusion

The particular choice of the risk parameter  $P_{\text{Exp}}$  and the runaway growth timescale defined in this paper is simply most convenient for the current model. One can imagine different metrics that similarly quantify the runaway debris growth risk. For instance, one could perform an exponential fit to the number of debris, i.e.,  $N_{\text{deb}} \propto \exp(t/\tau_{\text{exp}})$ , for the time values during which debris are experiencing run-away growth. In this case,  $\tau_{\text{exp}}$  represents the timescale of

exponential growth of debris. Another possible metric would be the probability of the number of debris surpassing a threshold. Specifically, this threshold  $N_{\text{deb,th}}$  can be the number of debris for which space becomes inoperable. The associated risk parameter can be defined as the fraction of simulated trajectories with  $N_{\text{deb}} > N_{\text{deb,th}}$  at time  $t$ , i.e.,  $P(t, N_{\text{deb}} > N_{\text{deb,th}})$ .

Since our stochastic simulations can be run relatively easily<sup>12</sup>, one can quickly explore various debris mitigation strategies (e.g., limiting launch rates, ADR). As an alternative to a quantity such as orbital carrying capacity [5, 7], one can use our risk parameter as a quantitative measure of the space environment's sensitivity to various actions. For example, as shown in this paper, one can calculate the projected risk of sustaining the current aggressive launch rate. Although various orbital capacity definitions can measure how close orbits are to being "full", they cannot provide a quantitative statement of the increased risk of runaway debris growth. In contrast, with our model and risk metric, one can quantify how an ASAT test increases the risk of runaway growth. Moreover, this risk parameter allows one to compare specific detailed mitigation strategies, given their costs [35] and the quantitative risk reduction (e.g., in terms of  $P_{\text{Exp}}$ ) that each provides.

There are several limitations to the model presented in this paper. First, we model the entire LEO region as a single volume, neglecting the altitude dependence of several processes. Second, although we try to choose reasonable values for the model parameters, these parameters are not well constrained in the current version. For example, one could calculate the debris decay rate from the effects of atmospheric drags and radiation pressure [36]. We leave the extension of our model to several altitude shells and the inclusion of more realistic models of the parameters to future work.

Unlike somewhat controllable launch and de-orbit timescales for satellites, the collision rate parameter described in Section 2 is less constrained, although it is commonly used in the literature. In particular, many PIB models calculate the collision probability under the assumption of random satellite motion. In reality, the motion of different satellites is correlated, as there are preferred orbits given a common set of mission objectives. Some authors have introduced a correction factor to account for this correlation [11], but it is unclear how well constrained this parameter is by empirical data. It is clear however, that collision probability has a huge impact in the future environment: the collision rate contributes to the growth of debris quadratically, while other processes (e.g., launch and decay) contribute linearly to debris growth. Figure (12) illustrates that different collision rates produce a large variation of runaway growth timescales. Therefore, we argue that the collision rate must be further theoretically and observationally constrained to provide better predictions of debris growth and the sustainability of space.

In summary, we have presented a statistical framework to describe the growth of orbital debris within the context of a source-sink evolutionary model. Our conclusions can be summarized as the following:

---

<sup>12</sup>No simulations shown in this paper required more than a few hours on a PC.

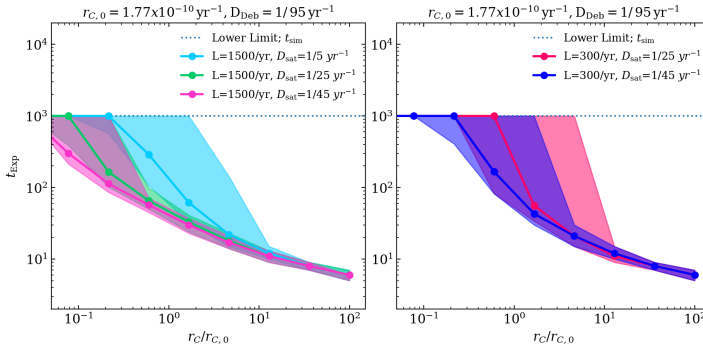


**Fig. 12** These figures show the variations in runaway growth timescale  $t_{\text{EXP}}$  as a function of the collision rate parameter, relative to a baseline value, for different values of the other parameters. One can see that more trajectories remain stable longer (i.e., higher  $t_{\text{EXP}}$ ) for smaller values of  $r_C/r_{C,0}$  and shorter satellite de-orbit timescales. The flattening of solid lines around the horizontal dotted line is an artifact due to the exponential timescales falling beyond the maximum time considered in the simulations ( $t_{\text{sim}} = 1000$  years). Similarly, the upper bound of color bands (90th percentile) sometimes extends beyond the end of simulations and is consequently truncated. If one allows the simulation to run, the high end of the  $t_{\text{EXP}}$  distribution would extend to higher value.

1. We introduce a risk parameter  $P_{\text{EXP}}$  that quantifies the risk of runaway debris growth. We show how one can assess the impacts of various processes on this risk metric. This metric could allow policymakers and engineers to perform quantitative cost-benefit analysis for various debris growth mitigation strategies.
2. We show the risk of runaway debris growth is sensitive to the number of lethal debris produced from each satellite breakup. Designing spacecraft to withstand impacts from small debris particles can therefore have a large impact on the future sustainability of space.
3. Although shortening the de-orbit rules for satellites can decrease the runaway debris growth risk and delay the onset of this growth, our model indicates that launching thousands of satellites every year may drive this risk to a significant level in the medium-term future.
4. Debris injection events, such as ASAT tests, have an appreciable impact on the long-term risk of runaway debris growth. The increase in probability depends on the amount injected and the state of the system at the time of debris injection.

We emphasize that these conclusions are drawn from a relatively simple source-sink model. Our primary goal in this paper was to introduce the stochastic framework for source-sink modeling, not to provide quantitative predictions on the near-term future of the Earth orbital environment. More precise and robust predictions would require improved modeling of the system and better constraints on the model parameters. For instance, adding altitude dependence to the model and better constraining the collision rate parameter would improve our model predictions. We leave these developments to future work.

**Acknowledgments.** We would like to thank Stephen Ouellette for the initial motivation for this project. We thank Jim Heagy, Joel Williamsen, Dan Pechkis, Jim Thorne, John Hong, Rachel Kuzio de Naray, Patrick Jafke, and Elena De La Rosa Blanco for thoughtful discussions. This project is funded by the Office of Developmental Test, Evaluation and Assessments (HQ0034-19-D-0001).

## References

- [1] 18th Space Defense Squadron. URL <https://www.space-track.org>
- [2] D.J. Kessler, B.G. Cour-Palais, Collision frequency of artificial satellites: The creation of a debris belt. *Journal of Geophysical Research: Space Physics* **83**(A6), 2637–2646 (1978). <https://doi.org/https://doi.org/10.1029/JA083iA06p02637>. URL <https://agupubs.onlinelibrary.wiley.com/doi/abs/10.1029/JA083iA06p02637>. <https://arxiv.org/abs/https://agupubs.onlinelibrary.wiley.com/doi/pdf/10.1029/JA083iA06p02637>
- [3] J.C. Liou, D. Hall, P. Krisko, J. Opiela, Legend - a three-dimensional leo-to-geo debris evolutionary model. *Advances in Space Research* **34**(5), 981–986 (2004). <https://doi.org/https://doi.org/10.1016/j.asr.2003.02.027>. URL <https://www.sciencedirect.com/science/article/pii/S0273117704000705>. Space Debris
- [4] H. Lewis, G. Swinerd, N. Williams, G. Gittins, in *Proceedings of the Third European Conference on Space Debris* (The European Space Agency (ESA), 2001), 473, pp. 373–378. URL <https://eprints.soton.ac.uk/21978/>
- [5] A. D’Ambrosio, M. Lifson, R. Linares. The capacity of low earth orbit computed using source-sink modeling (2022). <https://doi.org/10.48550/ARXIV.2206.05345>. URL <https://arxiv.org/abs/2206.05345>
- [6] D. Jang, A. D’Ambrosio, M. Lifson, C. Pasiecznik, R. Linares, in *Advanced Maui Optical and Space Surveillance Technologies Conference (AMOS)* (2022). URL <https://amostech.com/TechnicalPapers/2022/Space-Debris/Jang.pdf>
- [7] A. D’Ambrosio, M. Lifson, D. Jang, C. Pasiecznik, R. Linares, in *Advanced Maui Optical and Space Surveillance Technologies Conference (AMOS)* (2022). URL <https://amostech.com/TechnicalPapers/2022/Poster/D'Ambrosio.pdf>
- [8] C. Pasiecznik, A. D’Ambrosio, D. Jang, R. Linares. A dynamical systems analysis of the effects of the launch rate distribution on the stability of a source-sink orbital debris model (2022). <https://doi.org/10.48550/ARXIV.2212.01000>. URL <https://arxiv.org/abs/2212.01000>

- [9] G.L. Somma, Adaptive remediation of the space debris environment using feedback control. Ph.D. thesis, University of Southampton (2019). URL <https://eprints.soton.ac.uk/447843/>
- [10] H. Lewis, G. Swinerd, R. Newland, A. Saunders, The fast debris evolution model. *Advances in Space Research* **44**(5), 568–578 (2009). <https://doi.org/https://doi.org/10.1016/j.asr.2009.05.018>. URL <https://www.sciencedirect.com/science/article/pii/S0273117709003718>
- [11] D.L. Talent, Analytic model for orbital debris environmental management. *Journal of spacecraft and rockets* **29**(4), 508–513 (1992)
- [12] P. Fanto, Statistical properties of nuclei: Beyond the mean-field approximation. Ph.D. thesis, Yale University (2021)
- [13] S.X. Sun, G. Lan, E. Atilgan, in *Biophysical Tools for Biologists, Volume Two: In Vivo Techniques, Methods in Cell Biology*, vol. 89 (Academic Press, 2008), pp. 601–621. [https://doi.org/https://doi.org/10.1016/S0091-679X\(08\)00623-7](https://doi.org/https://doi.org/10.1016/S0091-679X(08)00623-7). URL <https://www.sciencedirect.com/science/article/pii/S0091679X08006237>
- [14] Q. Smith, E. Stukalin, S. Kusuma, S. Gerecht, S.X. Sun, Stochasticity and spatial interaction govern stem cell differentiation dynamics. *Scientific Reports* **5**(1), 12,617 (2015). <https://doi.org/10.1038/srep12617>
- [15] K.E. Johnson, A. Brock, Stochastic models for revealing the dynamics of the growth of small tumor populations. *bioRxiv* (2019). <https://doi.org/10.1101/743344>. URL <https://www.biorxiv.org/content/early/2019/08/22/743344>. <https://arxiv.org/abs/https://www.biorxiv.org/content/early/2019/08/22/743344.full.pdf>
- [16] P. Bittihn, R. Golestanian, Stochastic effects on the dynamics of an epidemic due to population subdivision. *Chaos: An Interdisciplinary Journal of Nonlinear Science* **30**(10), 101,102 (2020). <https://doi.org/10.1063/5.0028972>. URL <https://doi.org/10.1063/5.0028972>. <https://arxiv.org/abs/https://doi.org/10.1063/5.0028972>
- [17] S. Hussain, A. Zeb, A. Rasheed, T. Saeed, Stochastic mathematical model for the spread and control of corona virus. *Advances in Difference Equations* **2020**(1), 574 (2020). <https://doi.org/10.1186/s13662-020-03029-6>
- [18] L.J. Allen, A.M. Burgin, Comparison of deterministic and stochastic sis and sir models in discrete time. *Mathematical Biosciences* **163**(1), 1–33 (2000). [https://doi.org/10.1016/S0025-5564\(99\)00047-4](https://doi.org/10.1016/S0025-5564(99)00047-4). URL <https://www.sciencedirect.com/science/article/pii/S0025556499000474>

- [19] M. Assaf, M. Mobilia, E. Roberts, Cooperation dilemma in finite populations under fluctuating environments. *Phys. Rev. Lett.* **111**, 238,101 (2013). <https://doi.org/10.1103/PhysRevLett.111.238101>. URL <https://link.aps.org/doi/10.1103/PhysRevLett.111.238101>
- [20] M. Assaf, A. Kamenev, B. Meerson, Population extinction in a time-modulated environment. *Phys. Rev. E* **78**, 041,123 (2008). <https://doi.org/10.1103/PhysRevE.78.041123>. URL <https://link.aps.org/doi/10.1103/PhysRevE.78.041123>
- [21] D.T. Gillespie, A general method for numerically simulating the stochastic time evolution of coupled chemical reactions. *Journal of Computational Physics* **22**(4), 403–434 (1976). [https://doi.org/10.1016/0021-9991\(76\)90041-3](https://doi.org/10.1016/0021-9991(76)90041-3). URL <https://www.sciencedirect.com/science/article/pii/0021999176900413>
- [22] D.T. Gillespie, Approximate accelerated stochastic simulation of chemically reacting systems. *The Journal of Chemical Physics* **115**(4), 1716–1733 (2001). <https://doi.org/10.1063/1.1378322>
- [23] D.T. Gillespie, Stochastic simulation of chemical kinetics. *Annual Review of Physical Chemistry* **58**(1), 35–55 (2007). <https://doi.org/10.1146/annurev.physchem.58.032806.104637>
- [24] P. Lecca, Stochastic chemical kinetics. *Biophysical Reviews* **5**(4), 323–345 (2013). <https://doi.org/10.1007/s12551-013-0122-2>
- [25] G. Haag, *Modelling with the Master Equation* (Springer, Cham, Switzerland, 2017)
- [26] N. Johnson, P. Krisko, J.C. Liou, P. Anz-Meador, Nasa’s new breakup model of evolve 4.0. *Advances in Space Research* **28**(9), 1377–1384 (2001). [https://doi.org/https://doi.org/10.1016/S0273-1177\(01\)00423-9](https://doi.org/https://doi.org/10.1016/S0273-1177(01)00423-9). URL <https://www.sciencedirect.com/science/article/pii/S0273117701004239>
- [27] P.L. Houston, *Chemical kinetics and reaction dynamics* (Courier Corporation, 2012)
- [28] C. Collins, K. Senechal, Test and evaluation as a continuum. *The Journal of Test and Evaluation* **44**(1). URL <https://itea.org/journals/volume-44-1/test-and-evaluation-as-a-continuum/>
- [29] Federal Communications Commission. URL <https://www.fcc.gov/document/fcc-adopts-new-5-year-rule-deorbiting-satellites>
- [30] I.B. Schwartz, L. Billings, M. Dykman, A. Landsman, Predicting extinction rates in stochastic epidemic models. *Journal of Statistical Mechanics:*

- Theory and Experiment **2009**(01), P01,005 (2009). <https://doi.org/10.1088/1742-5468/2009/01/P01005>. URL <https://dx.doi.org/10.1088/1742-5468/2009/01/P01005>
- [31] A. Bongers, J.L. Torres, Star wars: Anti-satellite weapons and orbital debris. *Defence and Peace Economics* **0**(0), 1–20 (2023). <https://doi.org/10.1080/10242694.2023.2208020>. URL <https://doi.org/10.1080/10242694.2023.2208020>. <https://arxiv.org/abs/https://doi.org/10.1080/10242694.2023.2208020>
- [32] The White House. URL <https://www.whitehouse.gov/briefing-room/statements-releases/2022/04/18/fact-sheet-vice-president-harris-advances-national-security-norms-in-space/>
- [33] U.S. Space Command. URL <https://www.spacecom.mil/Newsroom/News/Article-Display/Article/2842957/russian-direct-ascent-anti-satellite-missile-test-creates-significant-long-last/>
- [34] United Nations Meeting Coverage and Press Releases. URL <https://press.un.org/en/2022/ga12478.doc.htm>
- [35] T.J. Colvin, J. Karcz, G. Wusk, Cost and benefit analysis of orbital debris remediation (2023)
- [36] J.C. Liou, N.L. Johnson, Risks in space from orbiting debris. *Science* **311**(5759), 340–341 (2006). <https://doi.org/10.1126/science.1121337>. URL <https://www.science.org/doi/abs/10.1126/science.1121337>. <https://arxiv.org/abs/https://www.science.org/doi/pdf/10.1126/science.1121337>